

Article

Fractioning Macrocomponents of *Nannochloropsis oceanica* by High-Pressure Homogenization, Membrane Processing, and Ethanolic Extraction

Pedro Cunha ^{1,2,3}, Bernardo Carvalho ^{1,3}, Mariam Kholany ^{1,3}, Helena Cardoso ² , Hugo Pereira ^{1,3} and João Varela ^{1,3,*} 

- ¹ GreenCoLab—Associação Oceano Verde, Universidade do Algarve, Campus de Gambelas, 8005-139 Faro, Portugal; pedrocunha@greencolab.com (P.C.); bernardocarvalho@greencolab.com (B.C.); mariamkholany@greencolab.com (M.K.); hugopereira@greencolab.com (H.P.)
- ² Allmicroalgae—Natural Products, Rua 25 de Abril, 2445-413 Alcobça, Portugal; helena.cardoso@allmicroalgae.com
- ³ Center of Marine Sciences, Universidade do Algarve, Campus de Gambelas, 8005-139 Faro, Portugal
- * Correspondence: jvarela@ualg.pt

Abstract

Multi-product biorefineries, which transform biomass feedstocks into multiple valuable bio-based products, are pivotal for transitioning from a fossil-based economy to a sustainable circular bioeconomy. This work proposes a processing pipeline for fractionating the macrocomponents of *Nannochloropsis oceanica*, which can serve as a basis for multi-product microalgae biorefineries. It consists of high-pressure homogenization (1200 bar, 1 cycle) to permeabilize the cells, and sequential membrane processing (0.2 μm dia-microfiltration followed by 100 kDa ultrafiltration) and ethanolic extraction (60 mL ethanol/g dry weight, 1 h) to fractionate the disrupted biomass. This biorefinery resulted in four final fractions: (1) enriched in water-soluble proteins ($39.0 \pm 2.8\%$ *w/w* proteins; $10.7 \pm 0.8\%$ *w/w* carbohydrates); (2) remaining soluble components ($5.7 \pm 0.4\%$ *w/w* proteins; $4.3 \pm 0.9\%$ *w/w* carbohydrates); (3) lipid-rich extract ($62.4 \pm 5.8\%$ *w/w* lipids); and (4) non-extracted components ($11.8 \pm 4.5\%$ *w/w* lipids), with mass recovery yields of $23.2 \pm 2.1\%$, $6.9 \pm 1.0\%$, $10.6 \pm 1.9\%$, and $60.4 \pm 4.1\%$, respectively. The ultrafiltration protein selectivity was not optimal, despite yielding a 2.6 times more concentrated fraction. Lipid extraction yield (35–60%) and purity (56–68%) were highly affected by the water content of the microfiltration retentate. Overall, $10.0 \pm 0.9\%$ of the proteins, $9.7 \pm 1.8\%$ of the carbohydrates, and $42.4 \pm 13.4\%$ of the lipids of *N. oceanica* were recovered in fractions 1, 2, and 3, respectively.

Keywords: microalgae; multi-product fractionation; mild processing; process integration; high-pressure homogenization; membrane filtration; ethanolic extraction



Academic Editor: Juan Luis Gomez Pinchetti

Received: 2 January 2026

Revised: 20 January 2026

Accepted: 23 January 2026

Published: 25 January 2026

Copyright: © 2026 by the authors.

Licensee MDPI, Basel, Switzerland.

This article is an open access article distributed under the terms and conditions of the [Creative Commons Attribution \(CC BY\)](https://creativecommons.org/licenses/by/4.0/) license.

1. Introduction

Microalgae are versatile bioresources with applications in various industries, including food and feed, nutraceuticals, cosmetics, chemicals, and materials, as well as services such as wastewater treatment and carbon sequestration. They are considered environmentally sustainable crops due to their low freshwater footprint, carbon dioxide consumption, and ability to grow on non-arable land [1]. However, as a highly technological industry, algae production costs are prohibitive for bulk commodities and are only economically viable for high-value specialty niche markets [2]. Biorefineries, which aim to valorize the majority

of biomass components, have emerged to bridge the gap between the production costs and the market value of microalgal biomass [3,4]. To date, most microalgae biorefineries are single-product or “high-value product first” biorefineries [5,6]. The focus is on optimizing the yield and purity of the chosen specialty ingredient, considering the remaining biomass fractions as by-products for low-value applications [7]. Only the target high-value biomass component is optimally valorized. However, for multi-component optimization, a cascading approach and process integration using a top-down integrative design are essential [6–8]. This systematic methodology considers all elements of the biomass, rather than optimizing individual components separately [8]. It enables co-product valorization and maximizes overall microalgal biomass revenue in multi-product biorefineries, contributing to an economically competitive microalgal industry and the creation of structured algae-based product value chains.

Nannochloropsis species (Eustigmatophyceae, Heterokontophyta) are recognized for being oleaginous microalgae, rich in lipids and polyunsaturated fatty acids, particularly eicosapentaenoic acid (EPA), a long-chain omega-3 fatty acid essential for human health. These algae also have a significant protein content, up to 50% of the biomass dry weight (DW), and water-soluble polysaccharides with immunostimulatory activity and potential biomedical applications [9,10]. Typically, processing *Nannochloropsis* biomass starts with lipid extraction, followed by valorization of the defatted biomass, particularly proteins [9,11–14]. However, organic solvents, commonly used in lipid extraction techniques, can denature proteins. Most water-soluble proteins become insoluble and lose their techno-functional properties [3]. For this reason, aqueous bioprocesses targeting the extraction of soluble biomass components first emerged as alternatives. In addition to preserving the functionality of compounds, using wet biomass as a feedstock avoids the energy-intensive, costly step of biomass drying. Conversely, the presence of water affects lipid extraction efficiency and increases the complexity of the process [15,16].

The first stage in aqueous-based biorefineries often involves breaking or permeabilizing microalgal cells to increase the extractability of water-soluble components. This is especially important for *Nannochloropsis* species, which have hard-to-break, thick, multilayered cell walls composed of ordered arrays of cellulose microfibrils, extensively cross-linked by hemicelluloses, and surrounded by algaenan, highly resistant aliphatic polymers [17–19]. Mechanical disruption, such as high-pressure homogenization (HPH) or bead milling, results in higher extraction yields than enzymatic hydrolysis and chemical treatments [20–23]. Unlike non-mechanical methods, it does not alter the native structure of biomolecules such as proteins and carbohydrates, provided mild processing conditions are maintained. Following cell disintegration/permeabilization, fractionation separates cellular contents into distinct components. Membrane filtration gained attention as a fractionation methodology because it is a chemical-free, low-energy, and mild process [24]. Some studies have reported the separation and purification of *Nannochloropsis* fractions enriched with water-soluble proteins [10,14,22] and carbohydrates [9]. Most studies targeting water-soluble *Nannochloropsis* biomass fractions (typically proteins) focus solely on the target high-value ingredients, failing to address the valorization of the remaining biomass components, such as the valuable lipid fraction. The same holds for studies targeting water-insoluble components (lipids and carotenoids), which also do not valorize water-soluble fractions [15,16,25,26]. A few publications have suggested multi-product fractionation for *Nannochloropsis* biomass, valorizing both the water-soluble and lipid fractions [7,27].

This work aimed to fractionate the macrocomponents of *Nannochloropsis oceanica* biomass and lay the foundation for future multi-product biorefineries. Energy-efficient, scalable processes, including HPH, membrane filtration, and ethanolic extraction, were selected. All processes were optimized under mild conditions to maximize yields and

sequentially integrated to preserve the functionality of cell components. Therefore, the focus was first on extracting water-soluble proteins and carbohydrates, and then on lipids in the water-insoluble fraction. Membrane fouling was quantified for the first time in the context of a *Nannochloropsis* biorefinery, in terms of total mass, proteins, and carbohydrates, by calculating mass balances for these components.

2. Materials and Methods

2.1. Microalga

Nannochloropsis oceanica CCAP 849/10 was supplied by Allmicroalgae—Natural Products as a concentrated frozen paste ($\approx 200 \text{ g L}^{-1}$). This biomass was cultivated under autotrophic conditions in a nutrient-replete medium in outdoor tubular photobioreactors at the company's production factory in Pataias, Portugal. After harvesting, the culture was pre-concentrated via membrane microfiltration (MF) ($0.2 \mu\text{m}$ membrane pore size) followed by centrifugation. The concentrated algae suspension was immediately frozen to preserve the biomass's original properties.

2.2. Cell Disruption/Permeabilization

Assuming that variations in cell concentration do not significantly affect the release of intracellular metabolites by HPH, pumpable, concentrated algae suspensions were used to reduce specific energy consumption [28]. Concentrated algae suspensions of *N. oceanica*, prepared at 100 g L^{-1} from the frozen paste, were subjected to HPH (1 cycle at 1200 bar) using a Panda Plus 2000 homogenizer (GEA Niro Soavi, Parma, Italy).

2.3. Evaluation of the Degree of Cell Disruption/Permeabilization

Cell disruption efficiency was assessed by quantifying the number of intact cells and the intracellular water-soluble metabolites released from cells before and after HPH. Indirect quantification methods were employed to measure these parameters. Cell integrity was evaluated by turbidity, measured as the optical density of the suspension at 750 nm. For quantification of intracellular water-soluble metabolites, the supernatant was measured for ultraviolet (UV) absorbance at 260 nm [29]. The supernatants were obtained by centrifuging the homogenized suspensions ($20,000 \times g$, 20 min, $20 \text{ }^\circ\text{C}$). Turbidity and UV absorbance were normalized to pre-homogenization values and expressed as relative values. The lower the relative turbidity was, the greater the number of damaged cells during HPH. The greater the relative UV absorbance is, the greater the quantity of intracellular water-soluble metabolites released during HPH.

2.4. Optimization of Cell Disruption/Permeabilization

The pressure and number of homogenization cycles, two key factors in the HPH process, were optimized using a face-centered central composite design in Design Expert 11 (Table 1). Despite being a discrete numeric variable, the number of cycles was treated as a continuous variable to facilitate the optimization process and limit the total number of runs, because cell disruption tends to vary smoothly with the number of homogenization cycles, following a logarithmic relationship [29]. Response surface methodology was used to correlate the effects of processing parameters on cell disruption efficiency. Few scenarios were simulated using the numerical optimization section of Design Expert 11 to optimize the disruption while maintaining as mild HPH conditions as possible by imposing certain conditions on the obtained second-degree polynomial model:

1. Maximizing the relative UV absorbance;
2. Maximizing the relative UV absorbance and minimizing the pressure and number of homogenization cycles;

3. Maximizing the relative UV absorbance and minimizing the relative turbidity.

Table 1. Experimental design matrix for high-pressure homogenization (HPH) optimization. A face-centered central composite design with five central points was used to construct the experimental matrix. The experimental conditions were tested randomly, not necessarily in the order listed below.

Condition	Pressure (bar)	Cycles
1	300	1
2	1200	1
3	300	3
4	1200	3
5	300	2
6	1200	2
7	750	1
8	750	3
9	750	2
10	750	2
11	750	2
12	750	2
13	750	2

2.5. Membrane Filtration

Membrane filtration systems with a filtration area of 0.35 m² (Vibro-Lab3500, Sani Membranes, Farum, Denmark) were used for homogenate fractionation. First, microfiltration (0.2 µm membrane pore size, PVDF, Synder Filtration, Vacaville, CA, USA) was used to remove cells and cell debris, yielding a clear permeate containing intracellular water-soluble compounds. The MF permeate was then processed by ultrafiltration (UF) using membranes with sequentially lower molecular weight cut-offs (MWCOs) of 100 and 10 kDa (PES, Synder Filtration, Vacaville, CA, USA) to fractionate the water-soluble compounds. All processes were performed at room temperature (~20 °C) under a constant permeate flux (12 L m⁻² h⁻¹ [10]) via a peristaltic pump at the permeate side of the membrane. The manometric pressure inside the membrane module was monitored during each filtration process and did not exceed 0.2 bar (much lower than the maximum manometric pressure of 3 bar allowed for the system). In the first version of the process, membrane filtration was performed as tangential flow filtration, followed by a final dead-end filtration to concentrate the retentate as much as possible. Then, the process was improved by removing the final dead-end filtration step and running the system in tangential flow mode throughout. A second improvement was implemented by operating the initial MF phase in diafiltration mode (two diavolumes of fresh water) and concentrating the retentate only then. The final version of the membrane fractionation process, consisting of dia-microfiltration followed by 100 kDa MWCO ultrafiltration, was performed in triplicate. Membrane cleaning consisted of an initial hot-water rinse (50 °C), followed by an alkaline detergent cleaning (50 °C, pH 10, 30 min) to remove organic matter attached to the membrane, an acid cleaning (50 °C, pH 2, 15 min) to remove inorganic deposits, and filling with a 20% *v/v* ethanol storage solution, as recommended by the supplier.

Membrane fouling was quantified using mass balances of total biomass, proteins, and carbohydrates, as the difference between the mass of the feed fraction (the homogenate in MF and the MF permeate in UF) and the sum of the masses of the permeate and retentate fractions obtained from each membrane filtration process.

2.6. Lipid Extraction

Ethanol (96% *v/v*) (Carlo Erba Reagents, Cornaredo, Italy) was used as the extraction solvent to obtain a high-value extract enriched with polar lipids and EPA, from water-

insoluble fractions (MF retentates). Different processing conditions were tested, including the solvent-to-biomass ratio (40- and 60-mL ethanol/g biomass DW) and extraction time (1 and 4 h) (Table 2). All extractions were performed at room temperature (25–30 °C).

Table 2. Operating conditions of the ethanolic extractions.

Extraction	Retentate Concentration (g L ⁻¹)	Retentate Lipid Content (% w/w)	Ethanol/Biomass Ratio (mL/g DW)	Time (h)
1	35	21	40	1
2	35	21	40	4
3	35	21	60	1
4	35	21	60	4
5	47	18	40	1
6	47	18	40	4
7	47	18	60	1
8	47	18	60	4

2.7. Biochemical Analysis

2.7.1. Carbohydrate Quantification

The total carbohydrate content was quantified via the phenol-sulfuric acid method [30]. A volume of 0.5 mL of phenol (5% *v/v*) was added to glass tubes containing an equal volume of the previously diluted fractions. Then, 2.5 mL of sulfuric acid (96% *v/v*) was added directly to the liquid surface, not the tube walls, to ensure good mixing. After 10 min, the samples were vortexed, incubated for 30 min, and then measured for absorbance at 490 nm. A calibration curve was prepared using glucose as the standard.

2.7.2. Protein Quantification

The nitrogen-to-protein conversion factor was used to estimate the total protein content of the water-insoluble fractions. The nitrogen content was determined by the Dumas combustion method using an organic elemental analyzer (Vario EL III, Elementar, Langensfeld, Germany) according to the manufacturer's procedure. The nitrogen-to-protein conversion factor used was 4.08 [31].

The protein content of the water-soluble fractions was quantified using the Pierce™ Modified Lowry Protein Assay Kit (Thermo Fisher Scientific, Waltham, MA, USA) according to the manufacturer's instructions, using bovine serum albumin as the standard.

2.7.3. Lipid Quantification

The lipid content was determined by gravimetric analysis using the Bligh and Dyer method [32] with slight modifications. Approximately 20 mg DW of previously lyophilized fractions was resuspended in 0.8 mL ultrapure Milli-Q® water and subjected to 3 cycles (1 min/cycle with 30 s intervals between cycles to prevent sample overheating) at 25 Hz in a mixer mill (MM400, Retsch, Haan, Germany). A mixture of solvents—methanol, chloroform, and ultrapure Milli-Q® water—at a 2:2:1.8 volume ratio was used to extract the lipids. After centrifugation at 2500 × *g* for 10 min, 0.5 mL of the chloroform fraction was transferred to pre-weighed tubes and placed overnight in a dry bath incubator (DBH 2 S000, IKA, Staufen, Germany) at 55 °C to evaporate the chloroform. The tubes were subsequently transferred to a desiccator for 3 h and weighed using a precision balance (MSA36S-000-DH, Sartorius, Göttingen, Germany). For the ethanolic extracts, no milling step was used. Instead, 10 mL of each extract was oven-dried overnight at 100 °C, followed by direct lipid extraction from the dry extract.

2.7.4. Dry Weight Quantification

The dry weight of every fraction was determined by placing pre-weighed plates with known sample volumes in an oven at 100 °C overnight. Plates were then transferred to a desiccator for at least 30 min before being weighed on a precision balance (GH-202, A&D Instruments, Abingdon, UK).

3. Results and Discussion

3.1. Cell Disruption/Permeabilization

The percentage of lysed cells was not quantified, as this would require knowledge of the processing conditions resulting in complete cell disruption. HPH disruption efficiency was assessed through increases in the relative UV absorbance of the homogenate supernatants and decreases in the relative turbidity of the homogenate (Figure 1). These two analytical methods are complementary: UV absorbance measures the release of water-soluble intracellular metabolites, and turbidity indicates the degree of cell damage. Scenario 1 was simulated to determine the optimal conditions for releasing intracellular components from the cell, regardless of the process intensity. The optimal HPH operating conditions should simultaneously maximize the relative UV absorbance and minimize the relative turbidity (scenario 3), ensuring the most efficient cell permeabilization with the mildest disruption procedure. The mildness of the HPH could also be simulated by minimizing pressure and the number of cycles (scenario 2). The polynomial models derived from the experimental results are shown in Table 3. Table 4 shows the simulation results for the three simulated scenarios. The two most promising scenarios (1 and 3) were later validated (Table 5). Interestingly, both the efficacy of intracellular metabolites release and the intensity of the homogenization process were considerably higher in the validation assay than in the optimization experiment. Several factors may explain the variability in results, such as the use of a different batch of biomass, regular maintenance of the equipment (including replacement of worn-out parts) performed between the two experiments, or simply the inherent process variability characteristic of bioprocesses. The second point is more likely the case because the homogenization blocks of high-pressure homogenizers wear out over time, which can affect cell disruption, particle size, and compound release. Because wear parts were not replaced between the optimization and validation trials, we believe this is the primary reason for the discrepancy observed. Regardless, it can be concluded that, despite the higher relative UV absorbance in scenario 1, scenario 3 provided the best compromise between process efficiency and intensity.

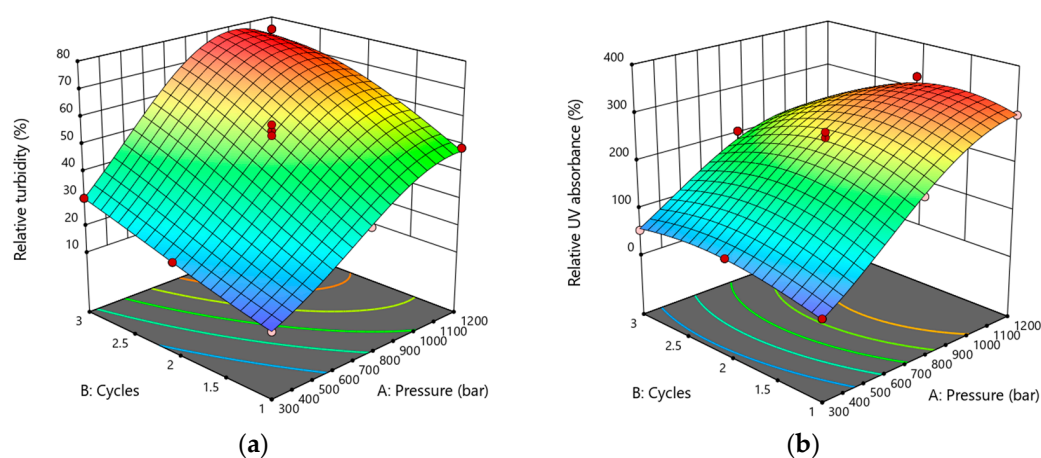


Figure 1. Surface response graphs showing (a) the level of cell damage and (b) the degree of intracellular metabolite release from the cells as functions of the HPH pressure and number of cycles. A 100% value represents the pre-homogenization cell conditions.

Table 3. ANOVA statistical analysis of the mathematical models derived from the experimental design. Each model fits each set of factors—pressure (P) and number of homogenization cycles (C)—with one response variable—relative UV absorbance (UV) and relative turbidity (T).

Response Variable	Relative UV Absorbance	Relative Turbidity
Model equation	$UV^{0.5} = -9.65 + 0.03P + 8.44C - 1.69C^2$	$\ln(T) = 0.18 + 1.08C - 0.11C^2$
Model <i>p</i> -value	<0.0001	<0.0001
<i>R</i> ²	0.9898	0.9958

Table 4. Summary of results from the different scenarios simulated using the numerical optimization module of the Design Expert 11 program, which employs the mathematical models built (one for each response variable) from the experimental data (Table 1) to explore the factor space and find the optimal combination of factor levels that meet the criteria set for each response and factor. The values obtained from simulations are purely theoretical and require experimental validation. The 1.6 cycles value in scenario 1 is a virtual value that must be rounded up for practical testing.

Scenario	Pressure (bar)	Cycles	Relative UV Absorbance (%)	Relative Turbidity (%)
1	1200	1.6	316	56
2	710	1.0	197	36
3	1200	1.0	302	46

Table 5. Validation of the two best scenarios identified using the optimization module of the Design Expert 11 program. Two homogenization cycles were performed in scenario 1 due to the impossibility of testing the 1.6 cycles suggested by the program. The results of both the optimization and validation experiments are shown. Values are the average and standard deviation of three replicates for the validation experiment.

Scenario	Experiment	Pressure (bar)	Cycles	Relative UV Absorbance (%)	Relative Turbidity (%)
1	Optimization	1200	2	327	62
	Validation			651 ± 9	56 ± 2
3	Optimization	1200	1	301	49
	Validation			550 ± 37	39 ± 1

Spiden et al. [29] advised that using UV absorbance to measure cell disruption should be approached with caution at high levels of cell rupture, as denatured metabolites could lead to an underestimation of the results. More specifically, the authors reported metabolite degradation in *Nannochloropsis* sp. at pressures greater than 1000 bar. Our results also suggest possible denaturation of the most sensitive biomass components, as shown by the reduction in UV absorbance from 2 to 3 HPH cycles at pressures above 750 bar (Figure 1). However, a single HPH cycle at 1200 bar does not seem to affect the integrity of the biomolecules. Depending on the quantification method used, reported cell disruption efficiencies vary considerably [33]. For example, Safi et al. [22] used flow cytometry quantification. They reported that approximately 90% and 97% of *Nannochloropsis gaditana* cells were lysed after one cycle of HPH at 1000 bar and 1500 bar, respectively. On the other hand, Bernaerts et al. [34] reported that, under similar conditions (1 HPH cycle at 1000 bar), turbidity and scanning electron microscopy indicated that the majority of *Nannochloropsis* sp. cells remained unaffected, with fewer than 20% disrupted. Spiden et al. [29] reported that only 33% of *Nannochloropsis* sp. cells were ruptured per homogenization cycle at the maximum pressure tested (1460 bar). The authors estimated that a homogenization pressure of 2000 bar would be required to achieve 50% rupture per pass. This significant

variability of results clearly highlights the absence of an infallible method for assessing cell disruption/disintegration. Additionally, preparing algae suspensions using dried, frozen, or fresh biomass is a variable that may significantly impact the results.

3.2. Membrane Filtration

Membrane filtration with different MWCOs was performed sequentially to fractionate the homogenate. Microfiltration, used to separate water-soluble from insoluble compounds, resulted in severe fouling (Figure 2), with more than half of the initial *N. oceanica* biomass accumulating on the membrane. This was a consequence of applying dead-end filtration at the end of the MF by completely closing the retentate valve and forcing the passage of the homogenate through the membrane. Despite inducing fouling, this approach maximized the permeate yields. A supplementary assay consisting of homogenate centrifugation ($7000 \times g$, 10 min) after the HPH was performed to actually quantify the relative quantity of water-soluble (supernatant) and insoluble (pellet) *N. oceanica* biomass components (Table 6). These results served as a reference for assessing bio-compound separation selectivity in membrane microfiltration, as the membrane may retain some intracellular water-soluble compounds released from the cells. Compared with the supplementary centrifugation assay results (Table 6), the MF mass-balance results indicated that most soluble compounds migrated to the permeate. However, the protein permeate yield was significantly lower than that obtained in the supplementary assay.

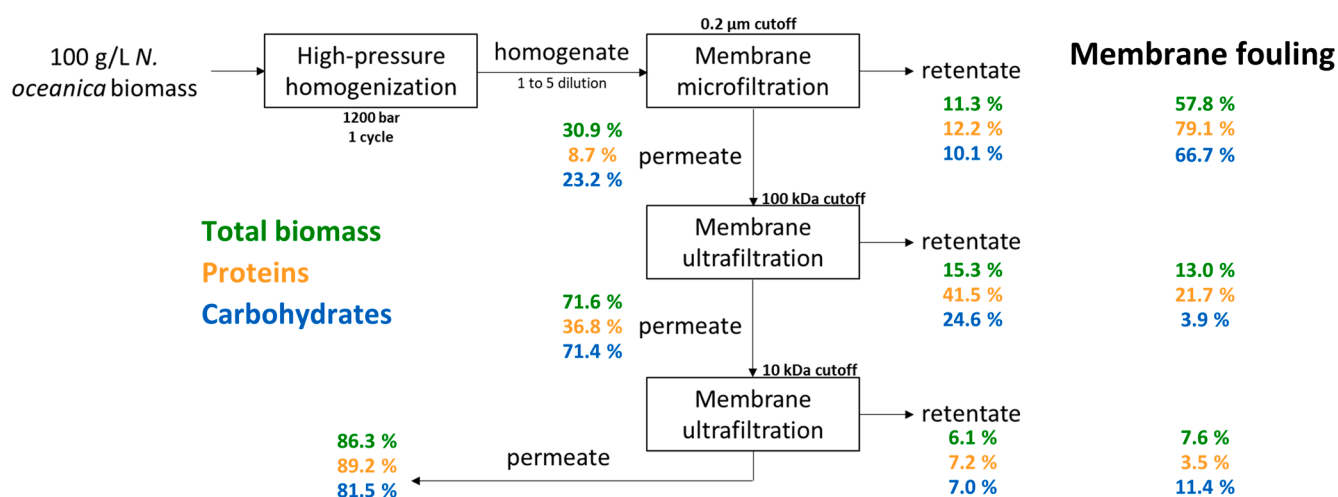


Figure 2. Total biomass (green, top), protein (orange, middle), and carbohydrate (blue, bottom) mass balances for the membrane fractionation process. The mass balances were calculated assuming each membrane filtration as a single process; i.e., the yields obtained are percentages of the total biomass, protein, and carbohydrate contents of the inlet fraction in each membrane process. For example, the 100 kDa ultrafiltration (UF) permeate yield is a percentage of the total biomass, protein, and carbohydrate content of the microfiltration (MF) permeate. All membrane filtrations were performed via tangential flow filtration, followed by final dead-end filtration. Membrane fouling is the mass difference between the inlet and outlet fractions in each filtration process. The values are shown as the average and standard deviation of three replicates of the membrane fractionation process.

Table 6. Fractionation of *Nannochloropsis oceanica* biomass into water-soluble and water-insoluble components. The homogenate was centrifuged ($7000 \times g$, 10 min), and the relative amounts of total biomass, proteins, carbohydrates, and lipids in the pellet and supernatant fractions were measured.

% of Partition	Total Biomass	Proteins	Carbohydrates	Lipids
Pellet	70.9	78.1	75.8	91.1
Supernatant	29.1	21.9	24.2	8.9

Following MF, 100-kDa MWCO ultrafiltration proved an effective method for separating proteins and carbohydrates from the MF permeate. While more than 70% of the carbohydrates present in the MF permeate were recovered in the UF permeate, only 37% of the proteins were co-extracted. Thus, a carbohydrate-enriched permeate and a protein-enriched retentate were obtained. Further purification of these two components was unsuccessful, as both proteins and carbohydrates were primarily found in the permeate after 10 kDa MWCO ultrafiltration. Consequently, this step was excluded from the fractionation process. As a separation technology based on molecular mass, UF fractionation efficiency is limited by differences in size between the components to be separated. The rules of thumb for good separation are that the molecular weights must differ by a factor of 10 and that the MWCO of UF membranes should be at least half the molecular weight of the solute to be retained [35]. Other authors suggested processing the supernatant obtained from a two-step centrifugation of *N. gaditana* homogenates using a 300 kDa MWCO membrane, followed by diafiltration, to separate polysaccharides from water-soluble proteins [7]. They considered that most proteins would migrate to the permeate, with carbohydrates retained by the membrane, contrary to what was observed in the present work. Interspecific variability in protein and carbohydrate profiles may explain such differences. Safi et al. [22] reported that after HPH and centrifugation, the protein profile of the supernatant from *Nannochloropsis gaditana* ranged from 40 to 720 kDa, with the largest band at 480 kDa.

The high level of fouling observed in the MF (Figure 2) is problematic for a fractionation process aiming to optimize biomass utilization. Thus, a few modifications were introduced to decrease membrane fouling. Instead of operating the filtration system in dead-end mode in the final part of the MF, tangential flow was maintained throughout the process (for both MF and UF). During MF, the pressure of the retentate side of the membrane was maintained between 0.1 and 0.15 bar (an increase from the 0 bar used in the original process) to expand the membrane cartridge and reduce fouling. Although these changes reduced fouling at the MF to approximately 2% of the homogenate DW, they also reduced the biomass permeate yield from 31 to 17%. Thus, a diafiltration (two diavolumes of freshwater) was introduced at the MF, preceding the concentration stage (Figure 3), to increase permeate yields. This maintained the feed concentration nearly constant and close to its initial value, growing only at the concentration stage.

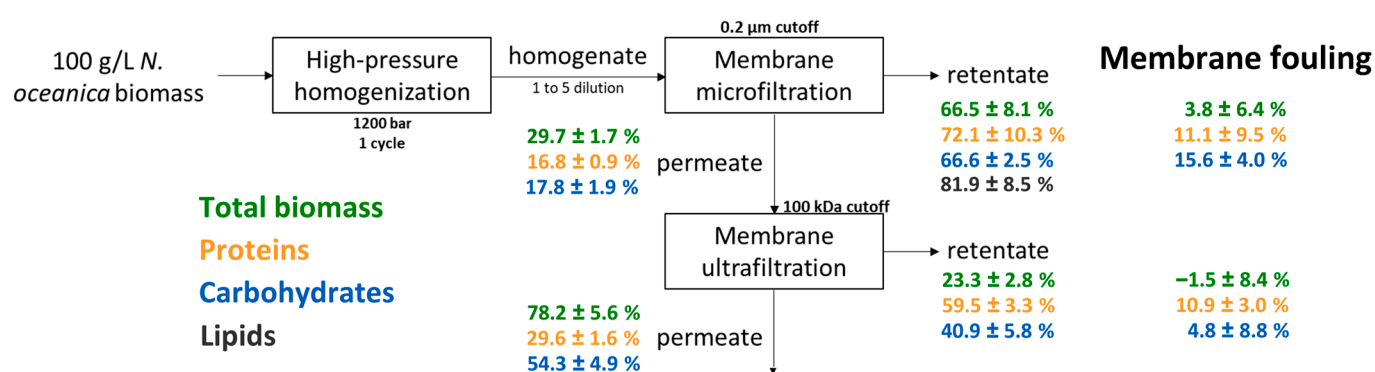


Figure 3. Total biomass (green, top), protein (orange, middle), carbohydrate (blue, bottom), and lipid (black, bottom for retentate of MF) mass balances for the modified membrane fractionation process. The mass balances were calculated assuming each membrane filtration as a single process; i.e., the yields obtained are percentages of the total biomass, protein, carbohydrate, and lipid contents of the inlet fraction in each membrane process. For example, the 100 kDa UF permeate yield is a percentage of the total biomass, protein, and carbohydrate content of the MF permeate. All membrane filtrations were performed as tangential flow filtrations. Membrane fouling is the mass difference between the inlet and outlet fractions in each filtration process. The values are shown as the average and standard deviation of three replicates of the modified membrane fractionation process.

The result was low fouling levels at MF ($4 \pm 6\%$ of the total inlet biomass, despite the high variability among replicates) and an increase in the permeate's biomass yield to $30 \pm 2\%$, matching the value of the original fractionation process (31%). The permeate protein yield ($17 \pm 1\%$) nearly doubled compared with the original method (9%), although the permeate carbohydrate yield ($18 \pm 2\%$) was lower than that in the original process (23%). Using Table 6 as a reference, approximately 75% of the water-soluble proteins and carbohydrates partitioned to the MF permeate. By performing diafiltration after the concentration phase, a common practice in microalgae biorefineries [14,22,36], the process becomes more prone to fouling, which affects the selectivity/retention of the membrane before diafiltration and jeopardizes the migration of soluble compounds through it [36]. Overall, the modifications introduced into the membrane fractionation process resulted in considerably higher protein retention during UF; however, protein–carbohydrate separation did not improve, as the permeate carbohydrate yield decreased compared to the original fractionation process.

Lysate clarification by centrifugation is performed to remove cells and cell debris, typically preceding membrane pressure-driven processes, which are primarily used in the pre-purification stage of high-value compounds [37]. This work proposed a complete membrane-based process for both clarification (0.2 μm MF) and fractionation (100 kDa MWCO UF). The permeate flow was maintained constant during MF and UF to avoid high fluxes at the start of the process, when the membranes were clean. This allows for precise control of the convective force near the membrane surface, reducing fouling, requiring less frequent and intensive cleaning, and extending the membrane's lifetime [10,22,38]. The unique setup of the fractionation process developed in this work hinders direct comparisons with similar works. Nevertheless, Safi et al. [22] reported $49 \pm 1\%$ soluble protein recovery in the supernatant after HPH (1500 bar, 1 cycle) and centrifugation, which was much greater than the value presented in Table 6 (21.9%) and even greater than the $16.8 \pm 0.9\%$ MF permeate protein yield (Figure 3). The same authors achieved a 17.4% protein permeate yield (from the total proteins of *N. gaditana* biomass) after a 300 kDa MWCO UF (using the supernatant from centrifugation as feed for membrane processing), followed by diafiltration under constant transmembrane pressure. In comparison, only $5.0 \pm 0.5\%$ of the initial proteins were detected in the UF permeate in this study. However, when the UF protein recovery out of the total proteins in the UF feed fraction was considered, the results were similar ($37.00 \pm 0.01\%$ for Safi et al. [22] and $29.6 \pm 1.6\%$ for this work). Ribeiro et al. [10] reported considerably higher protein permeate yields ($78.0 \pm 0.4\%$) with 100 kDa MWCO ultrafiltration starting with diafiltration. The relatively low protein levels in the UF permeate reported in the present work were due to inefficient cell disruption and the insoluble nature of some proteins in *Nannochloropsis* biomass [22]. Furthermore, it may also be owing to protein–protein or protein–debris aggregation that potentially formed during the overnight refrigerated storage (4 °C) of the homogenate, as suggested by Gifuni et al. [36]. The formation of large protein agglomerates through the aggregation of proteins with unequal charges may be another explanation [22]. Intensifying the HPH process or selecting a more specific disruption method, such as enzymatic hydrolysis with cellulase, could be an alternative to break the cellulose-rich *Nannochloropsis* cells and solubilize proteins and intracellular components.

To the authors' knowledge, this is the first time membrane fouling has been quantified not only in terms of total biomass but also in terms of proteins and carbohydrates adsorbed onto the membrane during *Nannochloropsis* processing. Fouling is typically evaluated qualitatively by measuring the reduction in permeate flow throughout the filtration process, rather than quantitatively. The exception was the work of Ribeiro et al. [10], which reported protein fouling of $7.42 \pm 0.40\%$ during 100 kDa MWCO ultrafiltration (with diafiltration

before the concentration stage), which is lower than the $10.9 \pm 3.0\%$ obtained in the present work.

3.3. Lipid Extraction

A significant portion of the initial biomass ($66.5 \pm 8.1\%$) was retained by the MF membrane and accumulated in the retentate (Figure 3). This retentate was composed of non-soluble cell proteins and carbohydrates, with most of the lipids ($81.9 \pm 8.5\%$) also present. Lipid extraction using ethanol as the extraction solvent was carried out and optimized (Figure 4). The extraction efficiency was primarily influenced by two factors: the solvent-to-biomass ratio and the characteristics of the retentate used as the extraction substrate. The extraction time had a relatively small effect on the process. The different DWs (35 and 47 g L^{-1}) of the two retentates used as substrates were critical for the efficiency of the ethanolic extractions. Despite the difference in water content between the two fractions being only 1.2% , the lipid extraction yields were at least 20% greater for the most concentrated retentate (47 g L^{-1}) under identical extraction conditions. The presence of water, a solvent miscible with ethanol, alters the polarity of the extraction solvent, influencing lipid mass transfer, which can be optimized by increasing the solvent-to-biomass ratio. A 50% increase in this variable resulted in a $15\text{--}28\%$ increase in lipid recovery. Given that the increases in total mass yields were not as significant as the lipid yields were, there was also an enhancement in the selectivity of the extraction, particularly when the least concentrated retentate was used as the substrate (35 g L^{-1}), since the ethanolic extracts obtained using $60 \text{ mL ethanol/g DW}$ were more than 10% richer in lipids than those obtained using $40 \text{ mL ethanol/g DW}$.

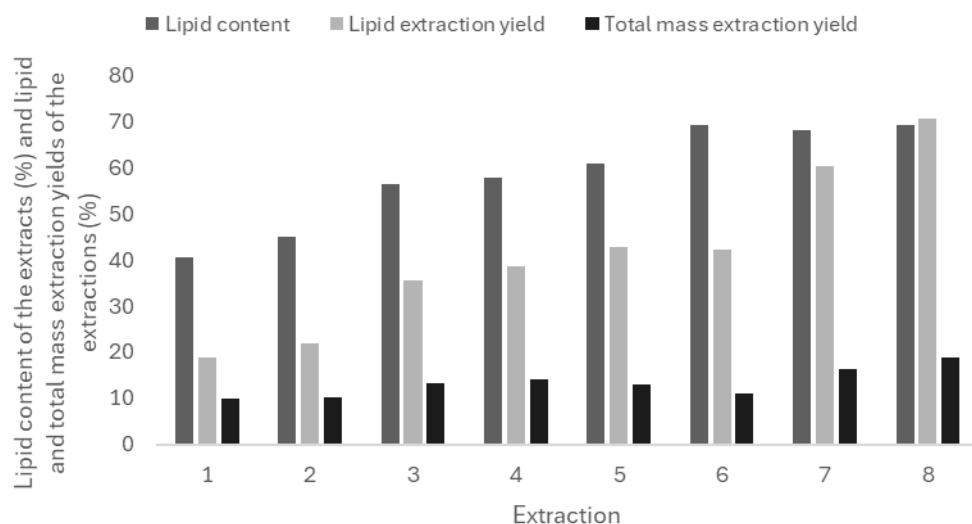


Figure 4. Mass and lipid extraction yields (out of the total mass of the MF retentate fraction) of the different ethanolic extractions carried out ($n = 1$), and lipid content of the produced extracts. The extraction conditions (Table 2) were as follows: (1 and 5) $40 \text{ mL ethanol/g DW}$, 1 h ; (2 and 6) $40 \text{ mL ethanol/g DW}$, 4 h ; (3 and 7) $60 \text{ mL ethanol/g DW}$, 1 h ; and (4 and 8) $60 \text{ mL ethanol/g DW}$, 4 h . Retentate 1 (35 g L^{-1} and 21% lipids) and retentate 2 (47 g L^{-1} and 18% lipids) were the substrates for ethanolic extractions 1 to 4 and 5 to 8, respectively.

Figueiredo et al. [39] and Ryckebosch et al. [40] reported mass extraction yields of 19.1% and approximately 30% from ethanolic extractions of *N. oceanica* and *N. gaditana*, respectively. Although the values ($9.8\text{--}18.7\%$) obtained in this work are lower, they were obtained using wet biomass as the extraction substrate, unlike in the two mentioned studies. Soto-Sierra et al. [13] achieved an even higher mass extraction yield (40%) in a two-step (45 min/step) wet lipid extraction using $50 \text{ mL ethanol/g DW}$ at $60 \text{ }^\circ\text{C}$. Nonetheless, lipid

extraction was performed on a *Nannochloropsis* sp. slurry with 20% solids, which was approximately five times more concentrated than in this work (3.5–4.7% solids). As a unit operation based on mass exchange between an aqueous feed and an organic solvent phase, wet lipid extraction is a biphasic system in which the solvent-to-biomass ratio and the water content of the extracted biomass are of paramount importance [41]. Yang et al. [42] identified the solvent-to-biomass ratio as the most influential variable for lipid extraction efficiency, followed by extraction time and temperature. Jiménez Callejón et al. [16] reported that the higher the ethanol-to-biomass ratio and the lower the water content, the higher the yield of saponifiable lipids. These authors demonstrated that subjecting *N. gaditana* suspensions to HPH before wet lipid extraction considerably improved saponifiable lipid recovery, highlighting the importance of preliminary cell disruption for solvent accessibility to lipids and reinforcing the need for cell disintegration processes for algae with rigid cell walls, such as *Nannochloropsis*.

The high solvent capacity of ethanol results in ethanolic extracts that are not pure lipid extracts, but also contain non-lipid components. Ryckebosch et al. [40] and Figueiredo et al. [39] reported that only 60% *w/w* and 42% *w/w* of the ethanolic extracts obtained from lyophilized *N. gaditana* and *N. oceanica* biomass consisted of lipids, respectively. These values are in the range of 40–70% *w/w* purities obtained in the present work. Furthermore, Ryckebosch et al. [40] reported a lipid extraction yield of 52%, which was higher than the lipid recovery values obtained in this work for all extractions except 7 and 8. Despite targeting the polar lipid fraction, Jiménez Callejón et al. [16] and Ryckebosch et al. [40] demonstrated that ethanolic extractions, whether performed under wet or dry conditions, result in greater neutral than polar lipid recoveries. To address the capacity of ethanol to extract both neutral and polar lipids, Jiménez Callejón et al. [15] proposed a simultaneous extraction and fractionation process to obtain EPA-rich polar lipid extracts from *Nannochloropsis* sp. biomass. The process consisted of a first hexane extraction to separate most neutral lipids, followed by an ethanolic extraction of the remaining biomass to extract the polar lipid fraction.

3.4. Overall Process Integration

A suitable biorefinery must be integrated with upstream processes to ensure the environmental and economic sustainability of the overall algae production process. Dewatering the diluted *Nannochloropsis* cultures harvested from the photobioreactors must therefore be optimized to achieve an algae paste with a concentration similar to that used during HPH (100 g L⁻¹). Further concentrating the culture to higher cell densities would require diluting the algae slurry before HPH, which is undesirable given that freshwater is increasingly scarce and valuable. Since the efficiency of HPH is independent of cell density, concentrating the culture to 20 g L⁻¹ to avoid a 5-fold dilution before microfiltration could be considered. However, because HPH is more energy-intensive than membrane filtration, the first scenario would be the most cost-effective. Harvesting 1 g L⁻¹ cultures, most of the energy would be used to concentrate it to 20 g L⁻¹, and only a small part would be used to concentrate it further to 100 g L⁻¹, because there is a 20-fold volume reduction in the first stage, which is much greater than the 5-fold concentration factor of the second phase.

A particularly important factor in the proposed fractionation process is the water content of the MF retentate, as the efficiency of the ethanolic extraction significantly depends on it, as mentioned earlier. Achieving a more concentrated retentate fraction at the end of the MF would significantly increase lipid extraction efficiency. This concentration would inevitably occur in a commercial-scale process, as the volume of processed homogenate would be substantially greater. Consequently, the homogenate concentration factor (or volume reduction factor) would increase significantly. However, the process must be

managed appropriately, as high concentrations on the retentate side of the membrane can cause fouling, compromising membrane retention and selectivity. Drying the MF retentate before lipid extraction may be an alternative to wet lipid extraction, with higher extraction efficiency. Furthermore, from an economic perspective, the energy consumption of recovering ethanol (a water-miscible solvent) via intensive distillation when wet extraction is employed could negate the benefits of avoiding drying [16].

The overall process developed for fractionating *N. oceanica* macrocomponents is represented in Figure 5. The biomass was fractionated into four final fractions: two water-soluble fractions, a lipid-rich extract, and a remaining fraction comprising all cellular content not solubilized in water or ethanol. The proposed fractionation methodology can potentially be integrated into multi-product biorefineries targeting both water-soluble and insoluble high-value products, such as soluble proteins or lipid extracts enriched in polyunsaturated fatty acids, particularly EPA. Transforming the water- and ethanol-soluble fractions in final products would require additional processing beyond the preliminary fractionation described in this work. Protein purification can be performed by protein precipitation (e.g., by adjusting the pH to near the isoelectric point [11] or by adding salts such as ammonium sulfate) or by high-resolution chromatographic techniques. Lipid extracts could be enriched in polar lipids by prior removal of the non-polar lipid fraction (using hexane [15], supercritical carbon dioxide [43], or silica gel chromatography [44]). Subsequently, polar lipid-rich extracts can be enriched in polyunsaturated fatty acids using methods such as winterization, urea complexation, chromatographic separation, molecular distillation, supercritical fluid fractionation or selective enzyme-catalyzed hydrolysis to obtain purified EPA extracts [45,46]. The additional fractionation processes would yield purer, potentially marketable ingredients; however, they would inevitably reduce overall product yield.

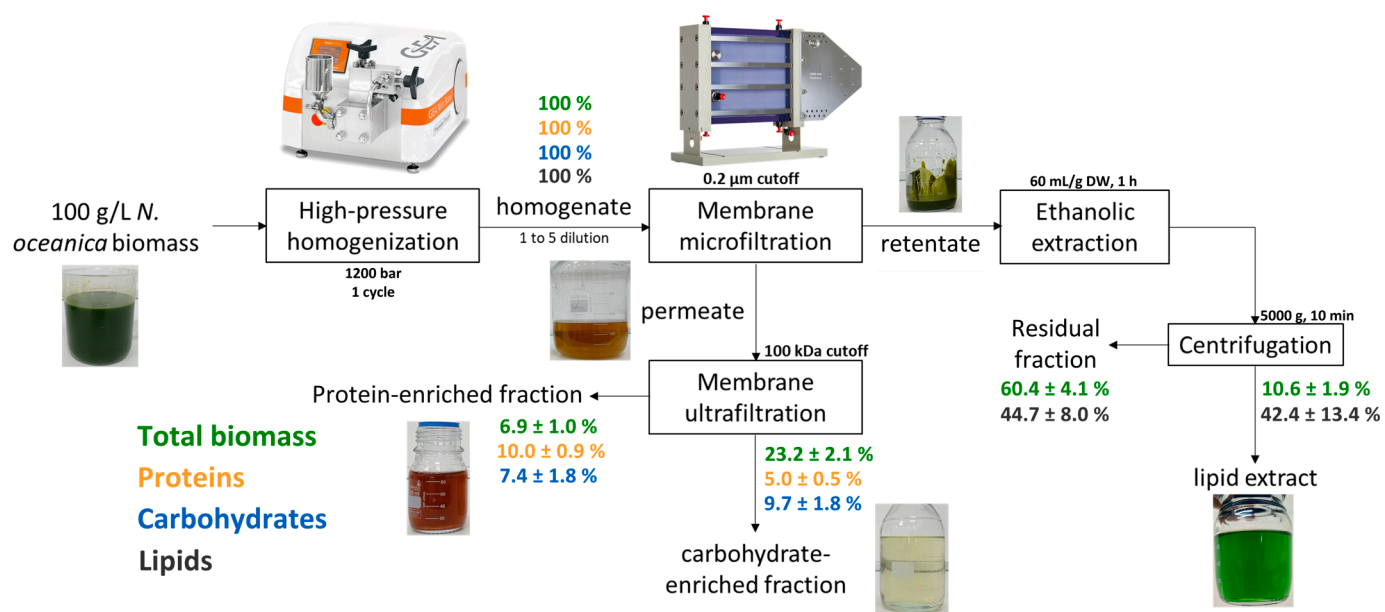


Figure 5. Final optimized fractionation process for *Nannochloropsis oceanica* and overall mass balances to total biomass (green), proteins (orange), carbohydrates (blue), and lipids (black). The mass balances were calculated treating the entire fractionation process as a single unit; thus, the yields represent percentages of the total biomass, protein, lipids, and carbohydrates in the homogenate. The values are shown as the average and standard deviation of three process replicates for membrane fractionation and two replicates for ethanolic extraction.

The nutraceutical value (essential amino acid content, digestibility, and bioactivity) of soluble proteins makes them suitable for food applications, especially when formulating

fortified foods, nutrition shakes, and sports drinks. Their functional properties (emulsification and foaming capacity) are desired in food formulations, such as soups, sauces, creams, or spreads [47]. Lipid-rich oil extracts from *Nannochloropsis* can be used as nutritional supplements for humans, providing EPA. This essential polyunsaturated fatty acid supports cardiovascular and mental health and has important anti-inflammatory properties [48]. The fraction containing the non-solubilized components still has a high protein and lipid content and likely significant amounts of EPA [12]. It could be used in aquaculture as a replacement for fish meal and fish oil in aquafeed, or in husbandry as animal feed [49]. This fraction accounts for $60.4 \pm 4.1\%$ and $44.7 \pm 8.0\%$ of the total processed biomass and lipids, respectively. Thus, the extraction of hydrophilic and lipophilic compounds could be improved. This could be achieved by intensifying the HPH process by increasing pressure (or eventually selecting a more specific cell disruption method, such as cellulose hydrolysis), increasing the solvent-to-biomass ratio, and/or increasing the lipid extraction temperature and/or time. Inevitably, this could be achieved at the expense of reducing the mildness and increasing the costs of the processes. Therefore, there must be a trade-off between process efficiency and costs, without forgetting the preservation of the products' structure/functionality. In addition, a more detailed biochemic analysis (e.g., amino acid and fatty acid profiling) will be needed in the near future to characterize each fraction fully, identify potential commercial applications, and design a comprehensive biorefinery pipeline for the production of purified, market-ready ingredients.

4. Conclusions

This work described the development of a process for fractionating the macromolecular components of *N. oceanica* biomass. Great emphasis was placed on process optimization and integration to maximize biomass utilization. The process began with one cycle of HPH at 1200 bar to permeabilize *Nannochloropsis* cells and release intracellular metabolites. Then, a 0.2 μm microfiltration separated most of the cellular water-soluble content into the permeate fraction, which was subsequently processed via 100 kDa MWCO ultrafiltration to segregate proteins (retentate) from carbohydrates (permeate). The remaining biomass was subjected to ethanolic extraction, yielding a lipid-rich extract (56–68% lipids) and a final fraction containing most of the initial biomass ($60.4 \pm 4.1\%$). The low extraction yields were probably due to the mildness of the biorefinery process, which may be relevant for preserving the original properties of the cell components.

To enhance the process, improvements to achieve higher permeate yields at the MF should be pursued. Increasing the HPH pressure and molecular weight cut-off of the microfiltration membrane could be a plausible way to do this. In addition, refining lipid extraction by separating polar from non-polar fractions could be an effective way to further valorize *Nannochloropsis* biomass. However, adding complexity to the fractionation process or intensifying it will increase production costs. Overall, the developed fractionation process can serve as a basis for future multi-product biorefineries aiming to valorize both water-soluble and insoluble fractions of *Nannochloropsis* biomass.

Author Contributions: Conceptualization, P.C. and H.P.; Methodology, P.C. and H.P.; Investigation, P.C.; Resources, H.P. and J.V.; Formal Analysis, P.C.; Data Curation, P.C.; Writing—Original Draft Preparation, P.C.; Writing—Review & Editing, P.C., B.C., M.K., H.C., H.P. and J.V.; Supervision, H.P. and J.V.; Project Administration, H.P. and J.V.; Funding Acquisition, H.P. and J.V. All authors have read and agreed to the published version of the manuscript.

Funding: This project was funded by Iceland, Liechtenstein, and Norway through the project MICROBOOST (PT-INNOVATION-0102—EEA.BG.CALL2.030.2021) and co-financed by Portuguese national funds from FCT—Foundation for Science and Technology through P.C.'s PhD fellowship (2021.08142.BD). This study received Portuguese national funds from FCT—Foundation for Sci-

ence and Technology through projects UIDB/04326/2020 (DOI:10.54499/UIDB/04326/2020) and LA/P/0101/2020 (DOI:10.54499/LA/P/0101/2020).

Data Availability Statement: All data supporting the findings of this study are included within the article.

Acknowledgments: The authors would like to acknowledge all the members of Allmicroalgae—Natural Products S.A., CCMAR, and GreenCoLab for their kind support and help. The authors are grateful to Allmicro-algae for generously donating the *N. oceanica* biomass samples.

Conflicts of Interest: Authors Pedro Cunha and Helena Cardoso were employed by the company Allmicroalgae–Natural Products. The remaining authors declare that the research was conducted in the absence of any commercial or financial relationships that could be construed as a potential conflict of interest.

Abbreviations

The following abbreviations are used in this manuscript:

EPA	Eicosapentaenoic acid
DW	Dry weight
HPH	High-pressure homogenization
UV	Ultraviolet
MF	Microfiltration
UF	Ultrafiltration
MWCO	Molecular weight cut-off

References

- Rajvanshi, M.; Sayre, R. Recent Advances in Algal Biomass Production. In *Biotechnological Applications of Biomass*; Basso, T., Basso, T., Basso, L., Eds.; IntechOpen: London, UK, 2021.
- Enzing, C.; Ploeg, M.; Barbosa, M.; Sijtsma, L. *Microalgae-Based Products for the Food and Feed Sector: An Outlook for Europe*; JRC Scientific and Policy Reports; European Commission: Luxembourg, 2017.
- Postma, P.R.; 't Lam, G.; Barbosa, M.J.; Wijffels, R.H.; Eppink, M.H.M.; Olivieri, G. Microalgal Biorefinery for Bulk and High-Value Products: Product Extraction within Cell Disintegration. In *Handbook of Electroporation*; Springer: Cham, Switzerland, 2017; Volume 3, pp. 2205–2224.
- Katiyar, R.; Banerjee, S.; Arora, A. Recent Advances in the Integrated Biorefinery Concept for the Valorization of Algal Biomass through Sustainable Routes. *Biofuels Bioprod. Biorefin.* **2021**, *15*, 879–898.
- Li, J.; Liu, Y.; Cheng, J.J.; Mos, M.; Daroch, M. Biological Potential of Microalgae in China for Biorefinery-Based Production of Biofuels and High Value Compounds. *New Biotechnol.* **2015**, *32*, 588–596. [[CrossRef](#)] [[PubMed](#)]
- Eppink, M.H.M.; Olivieri, G.; Reith, H.; van den Berg, C.; Barbosa, M.J.; Wijffels, R.H. From Current Algae Products to Future Biorefinery Practices: A Review. *Adv. Biochem. Eng. Biotechnol.* **2017**, *166*, 99–123. [[CrossRef](#)]
- Slegers, P.M.; Olivieri, G.; Breitmayer, E.; Sijtsma, L.; Eppink, M.H.M.; Wijffels, R.H.; Reith, J.H. Design of Value Chains for Microalgal Biorefinery at Industrial Scale: Process Integration and Techno-Economic Analysis. *Front. Bioeng. Biotechnol.* **2020**, *8*, 550758. [[CrossRef](#)]
- Diankristanti, P.A.; Hei Ernest Ho, N.; Chen, J.H.; Nagarajan, D.; Chen, C.Y.; Hsieh, Y.M.; Ng, I.S.; Chang, J.S. Unlocking the Potential of Microalgae as Sustainable Bioresources from up to Downstream Processing: A Critical Review. *Chem. Eng. J.* **2024**, *488*, 151124. [[CrossRef](#)]
- Pandeirada, C.O.; Maricato, É.; Ferreira, S.S.; Correia, V.G.; Pinheiro, B.A.; Evtuguin, D.V.; Palma, A.S.; Correia, A.; Vilanova, M.; Coimbra, M.A.; et al. Structural Analysis and Potential Immunostimulatory Activity of *Nannochloropsis oculata* Polysaccharides. *Carbohydr. Polym.* **2019**, *222*, 114962. [[CrossRef](#)]
- Ribeiro, C.; Santos, E.T.; Costa, L.; Brazinha, C.; Saraiva, P.; Crespo, J.G. *Nannochloropsis* sp. Biorefinery: Recovery of Soluble Protein by Membrane Ultrafiltration/Diafiltration. *Membranes* **2022**, *12*, 401. [[CrossRef](#)]
- Gerde, J.A.; Wang, T.; Yao, L.; Jung, S.; Johnson, L.A.; Lamsal, B. Optimizing Protein Isolation from Defatted and Non-Defatted *Nannochloropsis* Microalgae Biomass. *Algal Res.* **2013**, *2*, 145–153. [[CrossRef](#)]
- Chua, E.T.; Schenk, P.M. A Biorefinery for *Nannochloropsis*: Induction, Harvesting, and Extraction of EPA-Rich Oil and High-Value Protein. *Bioresour. Technol.* **2017**, *244*, 1416–1424. [[CrossRef](#)]

13. Soto-Sierra, L.; Wilken, L.R.; Mallawarachchi, S.; Nikolov, Z.L. Process Development of Enzymatically-Generated Algal Protein Hydrolysates for Specialty Food Applications. *Algal Res.* **2021**, *55*, 102248. [[CrossRef](#)]
14. Soto-Sierra, L.; Nikolov, Z.L. Feasibility of Membrane Ultrafiltration as a Single-Step Clarification and Fractionation of Microalgal Protein Hydrolysates. *Front. Bioeng. Biotechnol.* **2022**, *10*, 957268. [[CrossRef](#)] [[PubMed](#)]
15. Jiménez Callejón, M.J.; Robles Medina, A.; González Moreno, P.A.; Esteban Cerdán, L.; Orta Guillén, S.; Molina Grima, E. Simultaneous Extraction and Fractionation of Lipids from the Microalga *Nannochloropsis* sp. for the Production of EPA-Rich Polar Lipid Concentrates. *J. Appl. Phycol.* **2020**, *32*, 1117–1128. [[CrossRef](#)]
16. Jiménez Callejón, M.J.; Robles Medina, A.; Macías Sánchez, M.D.; Esteban Cerdán, L.; González Moreno, P.A.; Navarro López, E.; Hita Peña, E.; Grima, E.M. Obtaining Highly Pure EPA-Rich Lipids from Dry and Wet *Nannochloropsis gaditana* Microalgal Biomass Using Ethanol, Hexane and Acetone. *Algal Res.* **2020**, *45*, 101729. [[CrossRef](#)]
17. Zuorro, A.; Miglietta, S.; Familiari, G.; Lavecchia, R. Enhanced Lipid Recovery from *Nannochloropsis* Microalgae by Treatment with Optimized Cell Wall Degrading Enzyme Mixtures. *Bioresour. Technol.* **2016**, *212*, 35–41. [[CrossRef](#)]
18. Grossmann, L.; Ebert, S.; Hinrichs, J.; Weiss, J. Production of Protein-Rich Extracts from Disrupted Microalgae Cells: Impact of Solvent Treatment and Lyophilization. *Algal Res.* **2018**, *36*, 67–76. [[CrossRef](#)]
19. Maffei, G.; Bracciale, M.P.; Broggi, A.; Zuorro, A.; Santarelli, M.L.; Lavecchia, R. Effect of an Enzymatic Treatment with Cellulase and Mannanase on the Structural Properties of *Nannochloropsis* Microalgae. *Bioresour. Technol.* **2018**, *249*, 592–598. [[CrossRef](#)]
20. Safi, C.; Ursu, A.V.; Laroche, C.; Zebib, B.; Merah, O.; Pontalier, P.Y.; Vaca-Garcia, C. Aqueous Extraction of Proteins from Microalgae: Effect of Different Cell Disruption Methods. *Algal Res.* **2014**, *3*, 61–65. [[CrossRef](#)]
21. Safi, C.; Charton, M.; Ursu, A.V.; Laroche, C.; Zebib, B.; Pontalier, P.Y.; Vaca-Garcia, C. Release of Hydro-Soluble Microalgal Proteins Using Mechanical and Chemical Treatments. *Algal Res.* **2014**, *3*, 55–60. [[CrossRef](#)]
22. Safi, C.; Olivieri, G.; Campos, R.P.; Engelen-Smit, N.; Mulder, W.J.; van den Broek, L.A.M.; Sijtsma, L. Biorefinery of Microalgal Soluble Proteins by Sequential Processing and Membrane Filtration. *Bioresour. Technol.* **2017**, *225*, 151–158. [[CrossRef](#)]
23. Safi, C.; Cabas Rodriguez, L.; Mulder, W.J.; Engelen-Smit, N.; Spekking, W.; van den Broek, L.A.M.; Olivieri, G.; Sijtsma, L. Energy Consumption and Water-Soluble Protein Release by Cell Wall Disruption of *Nannochloropsis gaditana*. *Bioresour. Technol.* **2017**, *239*, 204–210. [[CrossRef](#)]
24. Gerardo, M.L.; Oatley-Radcliffe, D.L.; Lovitt, R.W. Integration of Membrane Technology in Microalgae Biorefineries. *J. Memb. Sci.* **2014**, *464*, 86–99. [[CrossRef](#)]
25. Nobre, B.P.; Villalobos, F.; Barragán, B.E.; Oliveira, A.C.; Batista, A.P.; Marques, P.A.S.S.; Mendes, R.L.; Sovová, H.; Palavra, A.F.; Gouveia, L. A Biorefinery from *Nannochloropsis* sp. Microalga—Extraction of Oils and Pigments. Production of Biohydrogen from the Leftover Biomass. *Bioresour. Technol.* **2013**, *135*, 128–136. [[CrossRef](#)]
26. Nirmala, N.; Arun, J.; Palanisamy, S.; Ravindran, R.S.E.; Abbas, M.; Kalathil, S.; Rahman, M.Z. Integrated Biodiesel and Biopolymer Production from *Nannochloropsis* Biomass: A Closed-Loop Biorefinery Approach. *RSC Adv.* **2025**, *15*, 42513–42521. [[CrossRef](#)]
27. Blanco-Llamero, C.; García-García, P.; Señoráns, F.J. An Integrated Biorefinery Process to Revalorize Marine Biomass from the Microalga *Nannochloropsis gaditana* Using Pressurized Green Solvents. *Mar. Drugs* **2025**, *23*, 263. [[CrossRef](#)] [[PubMed](#)]
28. Yap, B.H.J.; Dumsday, G.J.; Scales, P.J.; Martin, G.J.O. Energy Evaluation of Algal Cell Disruption by High Pressure Homogenisation. *Bioresour. Technol.* **2015**, *184*, 280–285. [[CrossRef](#)] [[PubMed](#)]
29. Spiden, E.M.; Yap, B.H.J.; Hill, D.R.A.; Kentish, S.E.; Scales, P.J.; Martin, G.J.O. Quantitative Evaluation of the Ease of Rupture of Industrially Promising Microalgae by High Pressure Homogenization. *Bioresour. Technol.* **2013**, *140*, 165–171. [[CrossRef](#)] [[PubMed](#)]
30. Dubois, M.; Gilles, K.A.; Hamilton, J.K.; Rebers, P.A.; Smith, F. Colorimetric Method for Determination of Sugars and Related Substances. *Anal. Chem.* **1956**, *28*, 350–356. [[CrossRef](#)]
31. Templeton, D.W.; Laurens, L.M.L. Nitrogen-to-Protein Conversion Factors Revisited for Applications of Microalgal Biomass Conversion to Food, Feed and Fuel. *Algal Res.* **2015**, *11*, 359–367. [[CrossRef](#)]
32. Bligh, E.G.; Dyer, W.J. A Rapid Method of Total Lipid Extraction and Purification. *Can. J. Biochem. Physiol.* **1959**, *37*, 911–917. [[CrossRef](#)]
33. Spiden, E.M.; Scales, P.J.; Kentish, S.E.; Martin, G.J.O. Critical Analysis of Quantitative Indicators of Cell Disruption Applied to *Saccharomyces cerevisiae* Processed with an Industrial High Pressure Homogenizer. *Biochem. Eng. J.* **2013**, *70*, 120–126. [[CrossRef](#)]
34. Bernaerts, T.M.M.; Gheysen, L.; Foubert, I.; Hendrickx, M.E.; Van Loey, A.M. Evaluating Microalgal Cell Disruption upon Ultra High Pressure Homogenization. *Algal Res.* **2019**, *42*, 101616. [[CrossRef](#)]
35. Singh, R. Introduction to Membrane Technology. In *Membrane Technology and Engineering for Water Purification*; Singh, R., Ed.; Elsevier: Amsterdam, The Netherlands, 2015; pp. 1–80.
36. Gifuni, I.; Lavenant, L.; Pruvost, J.; Masse, A. Recovery of Microalgal Protein by Three-Steps Membrane Filtration: Advancements and Feasibility. *Algal Res.* **2020**, *51*, 102082. [[CrossRef](#)]

37. Morales-Jiménez, M.; Yáñez-Fernández, J.; Castro-Muñoz, R.; Barragán-Huerta, B.E. Recovery of High Added Value Compounds from Microalgae Cultivation Using Membrane Technology. In *Membrane Separation of Food Bioactive Ingredients*; Jafari, S., Castro-Muñoz, R., Eds.; Springer: Cham, Switzerland, 2021; pp. 309–343, ISBN 9783030846435.
38. Miller, D.J.; Kasemset, S.; Paul, D.R.; Freeman, B.D. Comparison of Membrane Fouling at Constant Flux and Constant Transmembrane Pressure Conditions. *J. Memb. Sci.* **2014**, *454*, 505–515. [[CrossRef](#)]
39. Figueiredo, A.R.P.; da Costa, E.; Silva, J.; Domingues, M.R.; Domingues, P. The Effects of Different Extraction Methods of Lipids from *Nannochloropsis oceanica* on the Contents of Omega-3 Fatty Acids. *Algal Res.* **2019**, *41*, 101556. [[CrossRef](#)]
40. Ryckebosch, E.; Bermúdez, S.P.C.; Termote-Verhalle, R.; Bruneel, C.; Muylaert, K.; Parra-Saldivar, R.; Foubert, I. Influence of Extraction Solvent System on the Extractability of Lipid Components from the Biomass of *Nannochloropsis gaditana*. *J. Appl. Phycol.* **2014**, *26*, 1501–1510. [[CrossRef](#)]
41. Angles, E.; Jaouen, P.; Pruvost, J.; Marchal, L. Wet Lipid Extraction from the Microalga *Nannochloropsis* sp.: Disruption, Physiological Effects and Solvent Screening. *Algal Res.* **2017**, *21*, 27–34. [[CrossRef](#)]
42. Yang, F.; Xiang, W.; Sun, X.; Wu, H.; Li, T.; Long, L. A Novel Lipid Extraction Method from Wet Microalga *Picochlorum* sp. at Room Temperature. *Mar. Drugs* **2014**, *12*, 1258–1270. [[CrossRef](#)]
43. Jiménez Callejón, M.J.; Robles Medina, A.; Macías Sánchez, M.D.; González Moreno, P.A.; Navarro López, E.; Esteban Cerdán, L.; Molina Grima, E. Supercritical Fluid Extraction and Pressurized Liquid Extraction Processes Applied to Eicosapentaenoic Acid-Rich Polar Lipid Recovery from the Microalga *Nannochloropsis* sp. *Algal Res.* **2022**, *61*, 102586. [[CrossRef](#)]
44. Sánchez, M.D.M.; Callejón, M.J.J.; Medina, A.R.; Moreno, P.A.G.; López, E.N.; Cerdán, L.E.; Grima, E.M. Obtaining EPA-Rich Polar Lipids from Microalga *Nannochloropsis* sp. by Silica-Gel Chromatography Using Non-Toxic Solvents. *Biomass Convers. Biorefin.* **2022**, *13*, 15519–15530. [[CrossRef](#)]
45. Piyatilleke, S.; Thevarajah, B.; Nimarshana, P.H.V.; Ariyadasa, T.U. Large-Scale Production of *Nannochloropsis*-Derived EPA: Current Status and Perspectives via a Biorefinery Context. *Food Bioprod. Process.* **2024**, *148*, 255–268. [[CrossRef](#)]
46. Navarro López, E.; Jiménez Callejón, M.J.; Macías Sánchez, M.D.; González Moreno, P.A.; Robles Medina, A. Obtaining Eicosapentaenoic Acid-Enriched Polar Lipids from Microalga *Nannochloropsis* sp. by Lipase-Catalysed Hydrolysis. *Algal Res.* **2023**, *71*, 103073. [[CrossRef](#)]
47. Soto-Sierra, L.; Stoykova, P.; Nikolov, Z.L. Extraction and Fractionation of Microalgae-Based Protein Products. *Algal Res.* **2018**, *36*, 175–192. [[CrossRef](#)]
48. Kagan, M.L.; West, A.L.; Zante, C.; Calder, P.C. Acute Appearance of Fatty Acids in Human Plasma—A Comparative Study between Polar-Lipid Rich Oil from the Microalgae *Nannochloropsis oculata* and Krill Oil in Healthy Young Males. *Lipids Health Dis.* **2013**, *12*, 102. [[CrossRef](#)]
49. Moomaw, W.; Berzin, I.; Tzachor, A. Cutting Out the Middle Fish: Marine Microalgae as the Next Sustainable Omega-3 Fatty Acids and Protein Source. *Ind. Biotechnol.* **2017**, *13*, 234–243. [[CrossRef](#)]

Disclaimer/Publisher’s Note: The statements, opinions and data contained in all publications are solely those of the individual author(s) and contributor(s) and not of MDPI and/or the editor(s). MDPI and/or the editor(s) disclaim responsibility for any injury to people or property resulting from any ideas, methods, instructions or products referred to in the content.